Desalination and Water Treatment
www.deswater.com

doi: 10.5004/dwt.2023.29831

306 (2023) 122–130
September

Kinetic and equilibrium modeling of low-cost adsorbent of untreated watermelon peel for adsorption of zinc(II)

Nurul Izza Taib*, Nik Adriana Rosli, Mazwani Mohd Rejab, Nur Amira Farhana Mehamad Rosdi, Nurul Aqilah Abdul Aziz, Siti Noraihah Abd Halim

Faculty of Applied Sciences, Universiti Teknologi MARA, Perak Branch, Tapah Campus, 35400 Tapah Road, Perak, Malaysia, emails: izza257@uitm.edu.my (N.I. Taib), nikadrianarosli99@gmail.com (N.A. Rosli), mazwanivivo@gmail.com (M.M. Rejab), amirafarhanarosdi99@gmail.com (N.A.F. Mehamad Rosdi), nurulaqiesh19@gmail.com (N.A. Abdul Aziz), iamraihah@gmail.com (S.N. Abd Halim)

Received 31 March 2023; Accepted 8 August 2023

ABSTRACT

Watermelon peel is a bio-waste, lower cost, readily available, environment-friendly, and has high adsorption capacities. This study investigates the feasibility of dried watermelon peel (WP) as a low-cost adsorbent for removing Zn^{2+} from the aqueous solution. Batch experiments were conducted at different pH, initial concentrations, and contact times to evaluate dried watermelon peels' maximum adsorption capacity. The removal of Zn^{2+} was increased gradually with increasing pH, with the maximum removal observed at pH 5.0. Langmuir's model isotherm can well explain the equilibrium data for Zn^{2+} adsorption ($R^2 = 0.9812$). The monolayer adsorption capacity was found to be 20.45 mg/g at an optimum contact time of 1 h. Sorption energy analyses were conducted using Temkin and Dubinin–Radushkevich model isotherm. It was depicted that the sorption energies of Zn^{2+} on WP fitted well with the Dubinin–Radushkevich isotherm with $R^2 = 0.918$, indicating that the adsorption process is probably physical in nature. The adsorption kinetics shows that the pseudo-second-order equation could best explain the removal of Zn^{2+}. This study shows that the WP can potentially be an alternative low-cost adsorbent to remove Zn^{2+} from an aqueous solution.

Keywords: Watermelon peels; Zinc; Isotherm; Kinetics; Adsorbent

1. Introduction

As a result of the rapid industrial growth, the increasing discharge of polluted toxic heavy metals into environmental water bodies has caused a lot of serious pollution that affects people and other organisms. All the industrial wastewater released contains many heavy metals that are highly toxic and can harm aquatic creatures, are equally hazardous to human health, and therefore need to be treated [1]. For example, zinc is commonly released from the factory into the environment during mining and smelting activities that acidify the water. Exposure to high zinc levels over long periods may cause harmful effects such as vomiting, stomach cramps, and nausea [2]. According to WHO, the recommended concentration of Zn^{2+} for drinking water is 4.58×10^{-5} M due to problems associated with its organoleptic properties such as color, taste, and odor [3].

Many traditional methods have been done to remove heavy metals, including electrochemical treatment [4], chemical precipitation [5], membrane filtration [6], reverse osmosis [7], and ion exchange [8]. However, the adsorption method is considered the most convenient and effective way of pollutant removal due to its easy operation, low cost, and feasibility for large-scale applications [1]. Activated charcoal and nano sorbent have been explored as adsorbents for removing heavy metals, but they can be costly and difficult to regenerate [9]. Hence, the production of low-cost materials has been promoted to be used as suitable alternative

---

* Corresponding author.

adsorbents. Among these methods, the adsorption of metal ions using fruit peels such as lemon peel [10], mango peel [11], orange peel [12], banana peel [13], jack fruit peel [14,15], and watermelon peel [16] are preferred due to their lower costs, abandoned, readily available, environment-friendly biomaterial and high adsorption capacities.

The use of watermelon rind was studied by Shakor et al. [17], and maximum uptake of 52.81 mg/g was obtained. Yılmaz and Tugrul [18] reported six fruit peels that were chemically activated using $ZnCl_2$ and carbonized by microwave with zinc uptake of 39.18 mg/g for lemon, 35.78 mg/g for orange, 14.76 mg/g for watermelon, 13.06 mg/g for melon, 12.2 mg/g for pineapple and 9 mg/g for banana peels. Castro et al. [19], who also studied zinc adsorption by sodium hydroxide-activated and sodium hydroxide and calcium acetate-activated, achieved 25.59, 27.48, and 16.61 mg/g for banana, orange, and granadilla peels, respectively.

Watermelon peels (WP) are biomaterial waste and are easily available at no cost in plentiful amounts throughout tropical countries worldwide. The advantages of WP can be seen in their high metal uptake capacity and metal recovery due to the presence of pectin (carboxyl), citrulline, cellulose (hydroxyl), proteins, and carotenoid [20–22] which are easily bound to the metal ions [23]. Therefore, its conversion to potential low-cost adsorbents for wastewater treatment offers feasibility in the economy and handling of waste.

In the present study, untreated WP was evaluated to remove Zn^{2+} ions from the synthetic aqueous solution. The kinetics studies were assessed to comprehend the Zn^{2+} ion's adsorption mechanism onto the WP surface. The adsorption capacity was investigated by varying the contact time and initial Zn^{2+} concentration. The adsorption data were modeled with Langmuir, Freundlich, Dubinin–Radushkevich, and Temkin isotherms to study the adsorption process. Finally, WP was characterized using X-ray diffraction (XRD) and Fourier-transform infrared (FTIR) spectroscopy to characterize the watermelon peels.

2. Methodology

2.1. Preparation of untreated watermelon peel

Watermelon peels (WP) were collected from fruit stalls in Tapah, Perak, Malaysia. The watermelon peel (WP) was washed with distilled water, cut into small pieces, and dried in the oven for 24 h at 80°C. The dried peel was then cooled, cut into small pieces, and ground to obtain WP in fine powder form. The dried powder samples of WP were stored for further adsorption studies and characterization.

2.2. Preparation adsorbate

The stock solution of zinc ions (500 mg/L) was prepared by dissolving 1.0422 g of $ZnCl_2$ in 2 L of distilled water. A series of experimental solutions were prepared by diluting the stock solution to the certain concentrations needed.

2.3. Characterization

The functional groups of WP were obtained using a Perkin Elmer Spectrum One FTIR spectrophotometer (Perkin Elmer, Waltham, MA, USA) using the ATR technique. The FTIR spectra were recorded in a spectral region of 4,000–500 cm^{-1} with samples mounted on a diamond anvil at the resolution of 2 cm^{-1} and 10 scans were averaged to improve signal to noise ratio. The structure of the WP was carried out from X-ray powder diffraction (XRD). The intensity data were collected with a step size of 0.013° as a function of the Bragg angle, θ, in the range 2θ = 10° to 90° in Bragg–Brentano geometry using CuKα radiation wavelength $\lambda = 1.54$ Å (PANalytical's X'Pert PRO).

2.4. Batch adsorption studies

Adsorption isotherm experiments were performed in batch experiments. 0.20 g of dried WP was weighed into a 100 mL Erlenmeyer flask containing 50 mL of Zn^{2+} solutions with an initial concentration of 20–250 mg/L. The reaction mixture was shaken in the orbital shaker-incubator at 100 rpm for 4 h at 298 K. Kinetic studies were conducted in a continuously stirred flask containing 50 mL of Zn^{2+} solutions at 298 K by using the orbital shaker-incubator at 100 rpm at variable contact time (10–300 min) at a concentration of Zn^{2+} solutions (100 mg/L). In the study of the pH effect, only the pH of Zn^{2+} solutions was adjusted with 0.1 M HCl and 0.1 M NaOH. The supernatant of the reaction mixture was separated by filtration. The filtrate was analyzed using a flame atomic absorption spectrophotometer Perkin Elmer AAnalyst 400 (Perkin Elmer, Waltham, MA, USA). The percentage removal (%) and equilibrium adsorption capacity of WP (q_e, mg/g) were determined by Eqs. (1) and (2), respectively:

$$\text{Removal}\left(\%\right)=\frac{\left(C_o-C_e\right)}{C_o}\times 100 \tag{1}$$

$$q_e=\frac{\left(C_o-C_e\right)}{m}V \tag{2}$$

where q_e is the equilibrium adsorption capacity of WP (mg/g), C_o (mg/L) is the initial concentrations of Zn^{2+}, C_e (mg/L) is the final Zn^{2+} concentrations, V is the volume of the Zn^{2+} solution (L), and m is the weight of the WP (g).

3. Results and discussion

3.1. FTIR spectroscopy

Fig. 1a and b show the FTIR spectrum before and after the adsorption of Zn^{2+} on WP's surface, respectively. The

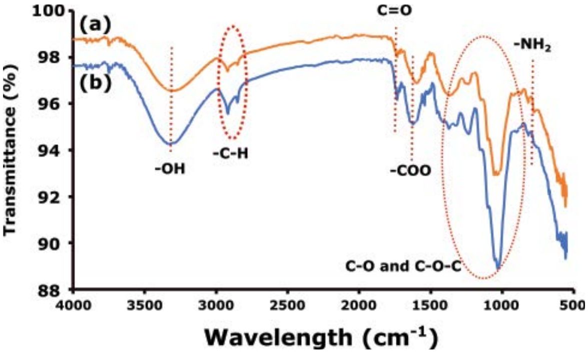

Fig. 1. Fourier-transform infrared spectra of (a) untreated watermelon peel and (b) Zn^{2+}-loaded watermelon peel.

intense and broad peak at 3,277 cm^{-1} (Fig. 1a) corresponds to –OH stretching vibrations (pectin and cellulose) of WP. The peak at 2,922 and 2,845 cm^{-1} represents the stretching vibrations of –C–H of the methyl and methoxy groups. The band at 1,736 cm^{-1} corresponds to C=O of the ester or carboxylic acid group, which may be from pectin. The band at 1,605 and 1,369 cm^{-1} characteristics of asymmetric and symmetric vibrations of –COO from carboxylic groups. Meanwhile, bands between 1,300 and 1,000 cm^{-1} are depicted to be C–O and C–O–C stretching vibrations in alcohols, ester, phenols, or carboxylic acid groups. The characteristic bands at 824 cm^{-1} indicated stretching vibrations of the $-NH_2$ group of proteins [16,24,25]. The shift of the FTIR peaks of WP from 3,277; 2,922; 2,845; 1,605; 1,369 and 824 cm^{-1} to 3,335; 2,918; 2,849; 1,616; 1,365 and 813 cm^{-1}, respectively (Fig. 1b) could be attributed to the adsorption of the Zn^{2+} on the surface of WP through electrostatic interaction. The shifting of peaks after loading the Zn^{2+} onto the WP indicated that oxygen-containing functional, carbonyl groups, and $-NH_2$ groups (Fig. 2) were involved in the adsorption of Zn^{2+} ions, which significantly removed Zn^{2+} from an aqueous solution.

Also, the n–d interactions occur (Fig. 3) between electron donor atoms (oxygen in carbonyl groups or nitrogen in amine groups on the adsorbent surface) and acceptors (free d orbitals in metal ions). This is supported by shifting the wavelength peak of FTIR from 1,605 to 1,616 cm^{-1}. Therefore, it is predicted that the adsorption of Zn^{2+} is produced due to both electrostatics and n–d mechanisms. These findings are consistent with Pearson's hard and soft acids and bases (HSAB) principle, which predicts that borderline cations Zn^{2+} will interact most strongly with the hard anion (O^-).

We could conclude from the putative adsorption mechanism presented in Figs. 2 and 3. Zn^{2+} is electropositive, whereas the WP has a lot of electronegative carboxyl groups. Zn^{2+} adsorption on the WP may be influenced by the electrostatic interactions between the cations and carboxyl anions. Whereas the functional groups $-NH_2$ are abundant in WP. The nitrogen atom has a high affinity for the cation. It makes sense that the nitrogen atoms on the WP surfaces could form strong complexes with Zn^{2+}, increasing the adsorption capability. The shifting in the intensity of –OH, carbonyl bands, and $-NH_2$ groups for the Zn^{2+} loaded WP confirms that they are the most active groups in WP and play a role in the adsorption process.

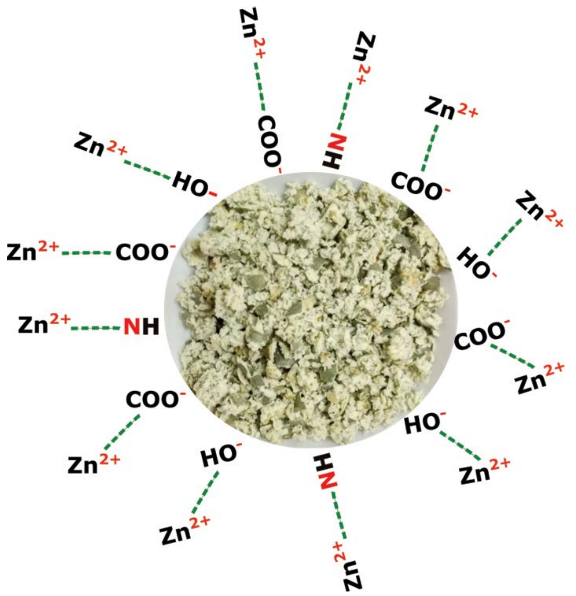

Fig. 2. Possible electrostatic interaction between COO^-, OH^-, and $-NH_2$ from watermelon peel surface with Zn^{2+}.

3.2. X-ray diffraction

The XRD diffraction pattern of WP before and after adsorption shows the difference in the absence of the peak, decreasing peak, and peaks' shifting. Fig. 4a shows the untreated WP's XRD. The intensity and sharpness of peaks indicate the untreated WP's semi-crystalline nature, with diffraction peaks appearing at 2q = 22.6°, 38.4°, 44.7°, 65.0°, and 78.2°. The XRD spectra of Zn^{2+} loaded WP showed a typical amorphous nature (Fig. 4b).

WP's crystalline nature changes to amorphous nature, indicating the adsorption of Zn^{2+} through electrostatic interactions between the positively charged (Zn^{2+}) and negatively charged ($-COO^-$ and OH) on the surface WP (Fig. 2). The carboxy or/and hydroxyl group were expected to be deprotonated, followed by the metal chelation. This also suggests that the adsorption has an adverse effect or alters the structure of WP, which is proven by the FTIR study. It is important to note that amorphous materials have more free space within their structure. They are often less dense than crystalline materials. This open space can take the shape of pores or voids, which can be linked or separated from one another and have the ability to absorb pollutants.

3.3. Determination of point of zero charge

In order to assess the interfacial characteristics of the WP, the pH at the point zero charges (pH_{pzc}) is measured. This feature determines which ionic species can be adsorbed by the WP at the appropriate pH. In 50 mL of 0.1 N sodium chloride (NaCl) as an electrolyte, a mass of 0.10 g of WP was added, and the pH of the electrolyte was

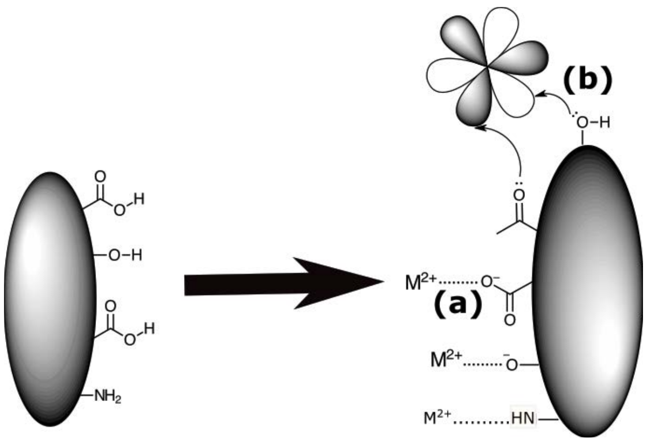

Fig. 3. Possible adsorption mechanisms of Zn^{2+}: (a) electrostatic attraction and (b) n–d interactions.

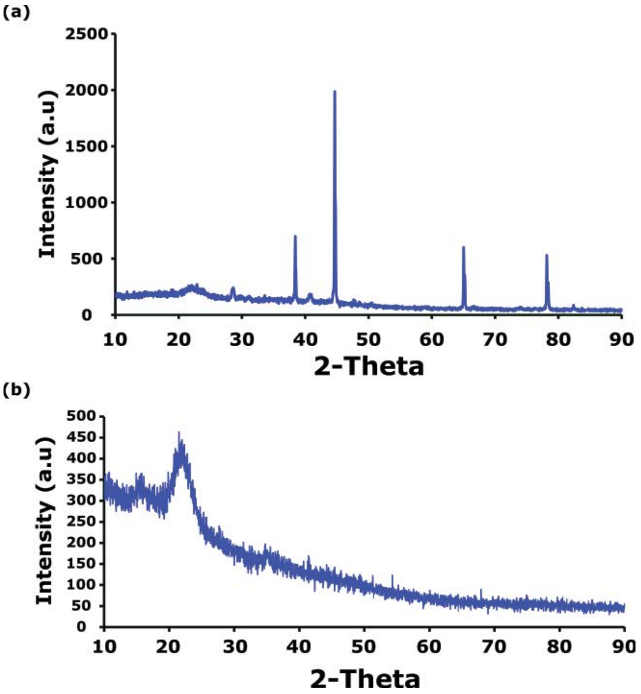

Fig. 4. XRD spectra of (a) untreated watermelon peel and (b) Zn^{2+}-loaded watermelon peel.

buffered to 2.00–12.00 by adding HCl (0.01 M) or NaOH (0.01 M). In order to determine the pH_{pzc} of the WP, a plot of the final pH minus the initial pH was plotted vs. the initial pH. The suspensions were then agitated for 24 h at room temperature, and the pH of each suspension was determined at the end of the experiment.

In Fig. 5, the pH_{pzc} of untreated WP was 6.40, indicating that the surface of WP was acidic, as can be observed from the results. Because of the presence of $–OH^-$ and $–COO^-$ groups on the surface of WP, the adsorption of Zn^{2+} has been attributed to these groups. This is consistent with the FTIR observations (Fig. 1), which show that carboxylic acids are present in high concentrations throughout WP. Because of protonation, the surface of WP is positively charged at pH values lower than 6.40 and negatively charged at pH values higher than 6.40. Hence, WP will more effectively adsorb cationic ions at pH values greater than 6.40. On the other hand, due to the electrostatic interactions, WP's adsorption of anionic species will be appropriate at pH values lower than 6.40.

3.4. Effect of pH

Fig. 6 illustrates the effect of pH on the adsorption of Zn^{2+} onto WP. The results show that the adsorption of Zn^{2+} onto WP increased gradually with an increase in solution pH up to pH 5.0, after which further increase in pH values exhibited minor decreases up to pH 8.0. The percentage removal increases from 70.6% at pH 3.0 to 92.1% at pH 5.0. Then it decreases to 80.3% at pH 6.0, which increases by increasing the pH to 8.0. Lower percentage removal at low pH may be due to excess H^+ ions competing with the Zn^{2+} for adsorption sites. In highly acidic conditions, the sorbents' major functional groups of binding sites are less ionized. Thus, the positive charge of metal ions is not captured by the negative charge of functional groups on the adsorbent surface. Moreover, the metal ions cannot bind to the active sites on the surface as the surface is completed by proton ions (H^+) [26].

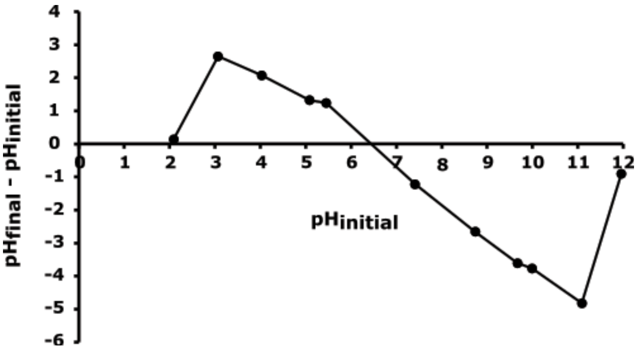

Fig. 5. Point of zero charges (pH_{pzc}) of the watermelon peel.

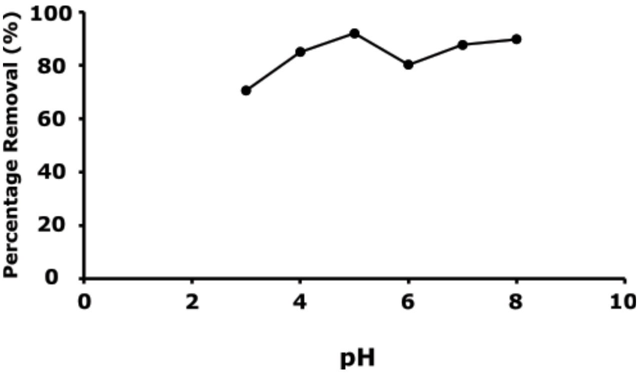

Fig. 6. Zn^{2+} percentage removal with different pH of the solution.

Moreover, at solution pH < pH_{pzc} = 6.40, the surface of WP was positively charged; thus, the repulsion between the Zn^{2+} and the positive surface of WP may have occurred and decreased the Zn^{2+} percentage removal. The low adsorption can be explained by the competition between metal ions and the high mobility of H_3O^+ ions, which compete for adsorption sites. Thus, the adsorption is reduced at low pH. At higher pH till the optimum, the surface of WP was likely to have negative surface charges due to the presence of functional groups as indicated by FTIR and became increasingly favorable for Zn^{2+} adsorption due to electrostatic forces of attraction between the negatively charged surface of the WP and Zn^{2+}. At pH 6.0, the adsorbent gives lower removal percentage, which may be due to the hydrolysis of Zn^{2+} forming the colloidal complex, which is very difficult to be adsorbed on the WP.

However, in this study, the optimum removal was observed at pH 5.0, lower than WP's pH_{pzc}. Therefore, it is suggested that the adsorption of Zn^{2+} onto WP could be governed via non-electrostatic interactions such as chemisorption and precipitation [27]. As a result, a pH of 5.0 was used for the following experiments.

3.5. Effect of initial concentration

Fig. 7 presents the removal percentage (%) of Zn^{2+} from an aqueous solution at different initial concentrations. It is evident that the Zn^{2+} percentage removal decreases significantly with the increase of initial Zn^{2+} concentration.

With a Zn^{2+} concentration of 50 mg/L, the percentage removal is at its maximum, with 95.2% removal, then gradually decreases, reaching 39.2% removal at 250 mg/L, consistent with prior studies [28]. Sufficient binding sites are available for more significant adsorption at lower concentrations due to the higher driving force. Meanwhile, at higher concentrations, the Zn^{2+} ions molecules compete with each other to be adsorbed on the binding sites of WP. Once the adsorption site becomes saturated, more Zn^{2+} ions are left unadsorbed in the solution. The Zn^{2+} removal percentage obtained in this study were higher than the previous report with $ZnCl_2$-activated carbon pomegranate peel (89%), H_2SO_4-activated carbon pomegranate peel (93%), $ZnCl_2$-activated carbon pineapple peel (93%), and H_2SO_4-activated carbon pineapple peel (93%) at a concentration of 40 mg/L [29].

3.6. Adsorption isotherm studies

The adsorption model isotherm is a powerful tool to relate the concentration of adsorbent in bulk and the amount of adsorbed at the interface at a constant temperature. In this work, adsorption equilibrium data were tested with Langmuir, Freundlich, Dubinin–Radushkevich, and Temkin models. The parameters of Langmuir, Freundlich, Dubinin–Radushkevich, and Temkin isotherm, along with regression coefficient R^2, are given in Table 1.

The Langmuir model assumes that the adsorption occurs as a monolayer with a homogeneous surface consisting of a finite number of binding sites with the adsorbed molecules that do not interact with each other. The Langmuir equation in linear form is represented as [28,30]:

$$\frac{C_e}{q_e} = \frac{1}{bq_{\max}} + \frac{C_e}{q_{\max}} \tag{3}$$

The equilibrium separation factor R_L, can be expressed by:

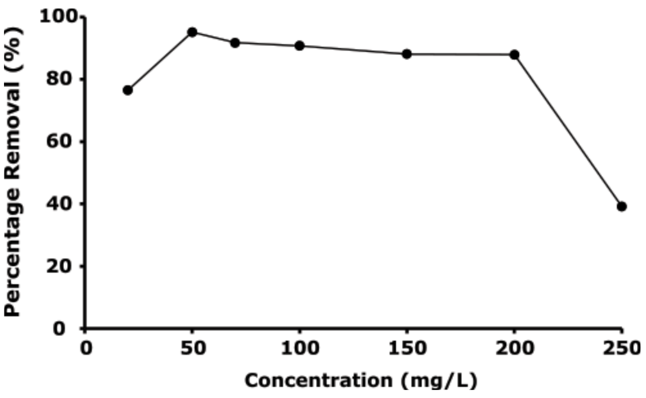

Fig. 7. Zn^{2+} percentage removal with different initial Zn^{2+} concentration.

$$R_L = \frac{1}{1 + bC_o} \tag{4}$$

The Freundlich isotherm assumes there is an interaction between the adsorbed molecules. Molecules are adsorbed on the adsorbent's heterogeneous surfaces based on different sites with irregular distribution of adsorption energies. The Freundlich adsorption isotherm in linear form is given as [28,31]:

$$q_e = K_F C_e^{1/n_F} \tag{5}$$

which can be simplified as:

$$\ln q_e = \ln K_f + \frac{1}{n_f} \ln C_e \tag{6}$$

The Dubinin–Radushkevich explains the experimental data on evaluating adsorbate's physical and chemical adsorbate based on its mean free energy E per molecule adsorbent. The equation is given as follows [32,33]:

$$\ln q_e = \ln q_D - \beta \left[RT \ln\left(1 + \frac{1}{C_e}\right) \right]^2 \tag{7}$$

$$\ln q_e = \ln q_D - \beta \in^2 \tag{8}$$

A straight line of $\ln q_e$ vs. ε^2 plot gives q_D as intercept and β as slope while the $\in$ (Polanyi potential) was calculated using:

$$\in = RT \ln\left(1 + \frac{1}{C_e}\right) \tag{9}$$

The E (kJ/mol) values refer to adsorption's free mean energy, which can be calculated using the following:

Table 1
Parameters derived from different isotherms for the adsorption of Zn^{2+} onto watermelon peel

Isotherm model	Estimated isotherm parameters	
Langmuir	$q_{\max}$	20.45 mg/g
	b	0.3903 L/mg
	R^2	0.9812
Freundlich	K_f	7.174 L/g
	n	3.060
	R^2	0.7891
Dubinin–Radushkevich	q_D	20.23 mg/g
	β	2×10^{-6} mol²/J²
	E	0.500 kJ/mol
	R^2	0.9180
Temkin	A_T	1.197 L/mg
	B	6.150 kJ/mol
	R^2	0.8417

$$E = \frac{1}{\sqrt{2\beta}} \tag{10}$$

The Temkin adsorption isotherm assumes that due to indirect interaction between absorbent–absorbate, all molecules have the heat of adsorption that would decrease linearly with the sorption coverage [13]. The equation can be described as follows:

$$q_e = \frac{RT}{b_T} \ln\left(A_T C_e\right) \tag{11}$$

The linear form of the isotherm in the linear form is expressed below:

$$q_e = B \ln A_T + B \ln C_e \tag{12}$$

with $B = RT/b_T$.
where q_e is the equilibrium Zn^{2+} concentration on the adsorbent (mg/g), C_e is the concentration of Zn^{2+} in the aqueous phase at equilibrium (mg/L), $q_{\max}$ (mg/g) is the maximum Zn^{2+} uptake (mg/g) of the adsorptive sites, b (L/mg) is the energy of adsorption (Langmuir constant), K_f (mg/g) is the sorbent's adsorption capacity, q_D is the maximum adsorption capacity (mg/g), β corresponds to mean adsorption energy (Dubinin–Radushkevich constant) (mol²/J²), B = Temkin constant associated with the heat of sorption (J/mol), A_T = Temkin equilibrium binding constant corresponding to the maximum bonding energy (L/mg), b_T = Temkin isotherm constant, R = gas constant (8.314 J/mol·K), T = 298.15 K.

The values b and $q_{\max}$ shown in Table 1 can be derived from the intercept and slope of the linear plots (Fig. 8), respectively. The correlation coefficient value was found to be 0.9812, suggesting that the adsorption of Zn^{2+} onto WP takes place in monolayer coverage on the homogeneous surface of the WP. This indicates that each Zn^{2+} molecule/WP has equal adsorption activation energy [24,34]. The WP's calculated monolayer capacity ($q_{\max}$) for the Zn^{2+} is comparable to the maximum adsorption obtained experimentally (19.80 mg/g).

The effectiveness of the adsorption process can be determined by the value range of: unfavourable ($R_L > 1$), linear ($R_L = 1$), favorable ($0 < R_L < 1$), and irreversible ($R_L = 0$). The R_L factor values fall in the range of 0–1, suggesting the favorable adsorption of Zn^{2+} onto WP. The decreasing R_L values with the increasing concentrations are proposed to improve the adsorption process at the higher initial concentration of Zn^{2+} [35].

The $n_F > 1$ provides the favorability of adsorption. The K_f and n_F can be calculated from the intercept and slope of the linear plot of $\ln q_e$ vs. $\ln C_e$ in Fig. 9. Table 1 shows $K_f = 7.174$ L/g, $n_F = 3.060$, and $R^2 = 0.7891$. The magnitude of K_f and n_F established an easy removal of Zn^{2+} from the aqueous solution. Thus, the Zn^{2+} adsorption process using WP can be considered favorable [36] and indicates that physisorption has occurred [37]. However, it was found that the correlation coefficient was ≤0.99, indicating that the Freundlich model cannot be applied to the present study.

Based on the correlation coefficient (R^2), isotherms Langmuir can describe the adsorption well. Thus, there is the possibility that monolayer adsorption and physisorption governed the adsorption of Zn^{2+} onto the WP.

Meanwhile, the following values for the Dubinin–Radushkevich model were estimated: q_D = 20.23 mg/g, $\beta = 2 \times 10^{-6}$ mol²/J² (Fig. 10), indicating a physical adsorption process in the $R^2 = 0.9180$.

The adsorption process is said to be physisorption for the $E < 8$ kJ/mol, the range of $8 < E < 16$ kJ/mol indicates

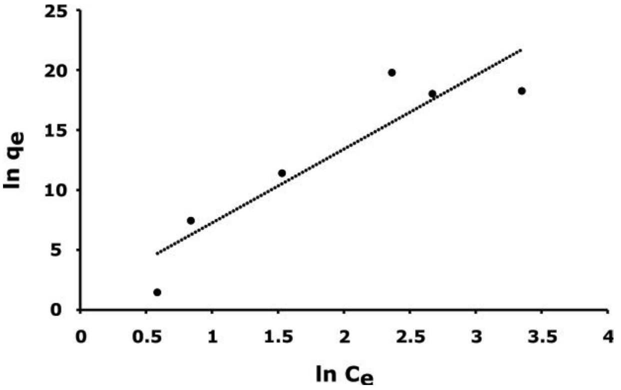

Fig. 9. Freundlich plot for the adsorption of Zn^{2+} onto watermelon peel.

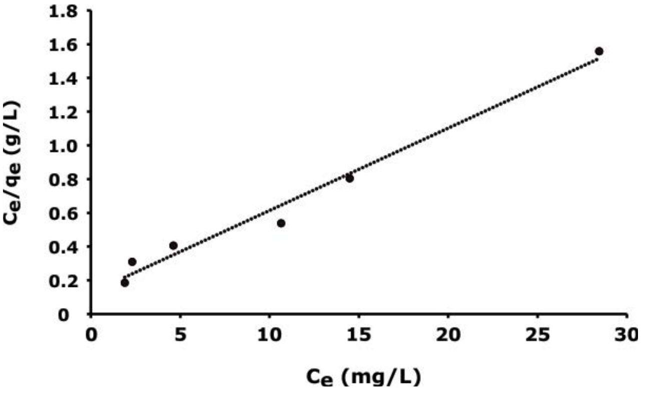

Fig. 8. Langmuir plot for the adsorption of Zn^{2+} onto watermelon peel.

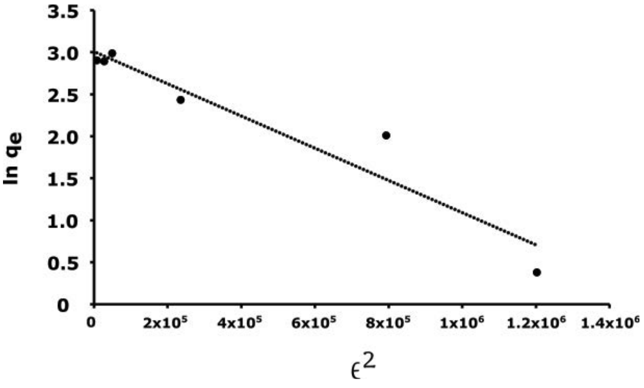

Fig. 10. Dubinin–Radushkevich plot for the adsorption of Zn^{2+} onto watermelon peel.

chemical ion-exchange mechanism takes place, and by chemical particle diffusion $E > 16$ kJ/mol [38]. The E obtained (0.5 kJ/mol) was less than 8 kJ/mol, suggesting adsorption of Zn^{2+} onto WP, which generally involves weak van der Waals forces between adsorbates and adsorbents; an indication of physisorption dominates the adsorption process.

Meanwhile, for the Temkin model, the A_T and B can be determined by plotting q_e vs. $\ln C_e$. From the Temkin plot (Fig. 11), the following values were estimated: $A_T = 1.197$ L/mg and $B = 6.150$ kJ/mol, indicating that the adsorption of Zn^{2+} onto WP occurred via physisorption with $R^2 = 0.8417$. The constant value was found to be <8 kJ/mol. This indicates that the Zn^{2+} interacts on the surface of WP only through weak van der Waals interactions associated with relatively low adsorption energies [39]. Based on Fig. 9, it can be concluded that the heat of adsorption increased linearly for WP. The Dubinin–Radushkevich model with a higher correlation coefficient value, $R^2 = 0.918$, proves a better choice to explain sorption energies, indicating a physical adsorption process.

3.7. Effect of contact time

Fig. 12 shows the percentage removal (%) at different contact times, indicating that the adsorption of Zn^{2+} was rapid. Adsorption increases from 87.39% for 10 min of exposure up to 92.89% for 240 min. The removal of Zn^{2+} was not significantly affected by the increasing contact time, aligned with the previous work [40], suggesting the saturation state had been reached. The large concentration gradient between the bulk solution and the adsorbent surface influences the rapid adsorption rate. The availability of vacant adsorption sites on the WP surface increases the Zn^{2+} uptake, becoming occupied until it reaches equilibrium.

3.8. Adsorption kinetic studies

For adsorption kinetics studies, it is related to contact time as it plays an essential role in affecting adsorption efficiency. Therefore, the kinetic of Zn^{2+} adsorption on WP was modeled with pseudo-first-order and pseudo-second-order models. The pseudo-first-order rate equation of Langergen is shown as [40]:

$$\log\left(q_e - q_t\right) = \log q_e - \frac{k_1}{2.303}t \tag{13}$$

The pseudo-second-order equation can be expressed as [40]:

$$\frac{t}{q_t} = \frac{1}{k_2 q_e^2} + \frac{t}{q_e} \tag{14}$$

where q_e is the concentration of Zn^{2+} on the adsorbent at equilibrium (mg/g), q_t is the concentration of Zn^{2+} on the adsorbent at time t, k_1 is the reaction rate constant of pseudo-first-order, and k_2 is the reaction rate constant of pseudo-second-order. A plot of the $\log(q_e - q_t)$ vs. t plot gives k_1 the intercept and theoretical $q_{e,\text{cal}}$ as the slope. The derived intercept and slope from the linear plot of t/q_t vs. t plot give k_2 and theoretical $q_{e,\text{cal}}$ values, respectively (Fig. 13).

Additionally, the strong agreement between q_e values obtained from the pseudo-second-order model (6.02 mg/g) and the experimental values (6.14 mg/g) confirmed this model's suitability in explaining the adsorption on the WP (Table 2). The second-order rate constant (k_2) value was 0.080 g/mg·min. These results indicate that the adsorption of Zn^{2+} onto WP is more likely to be controlled by the chemisorption process [41,42].

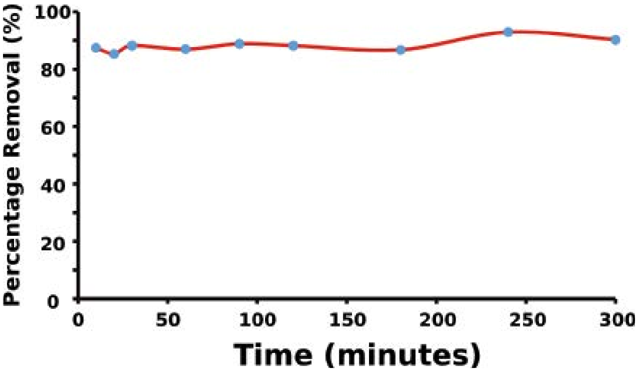

Fig. 12. Zn^{2+} percentage removal with contact time.

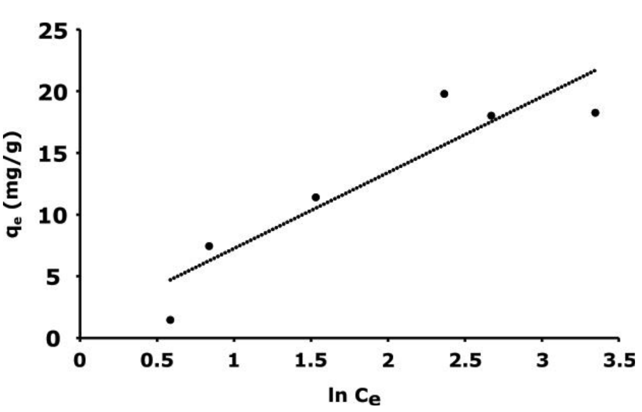

Fig. 11. Temkin plot for Zn^{2+} removal from aqueous solutions by watermelon peel.

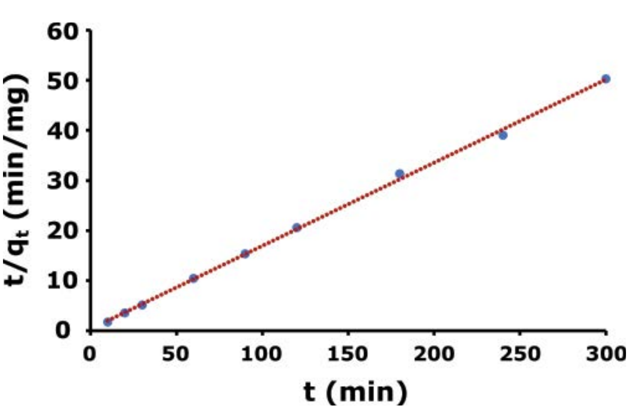

Fig. 13. Pseudo-second-order kinetics for the adsorption of Zn^{2+} onto watermelon peel.

Table 2
Adsorption kinetic parameters for the removal of Zn^{2+} by using watermelon peel

Pseudo-first-order			Pseudo-second-order			
R^2	k_1 (min^{-1})	$q_{e,cal}$ (mg/g)	R^2	k_2 (g/mg·min)	$q_{e,cal}$ (mg/g)	$q_{e,exp}$ (mg/g)
0.916	0.019	34.2	0.999	0.080	6.02	6.14

Table 3
Comparative of adsorption capacities for Zn^{2+} onto different biomass materials

Adsorbents	Adsorption capacities (mg/g)	References
Banana peel	25.59	[19]
Orange peel	27.48	[19]
Granadilla	16.61	[19]
Orange peel	21.25	[43]
HNO_3 treated orange peel	5.25	[44]
HNO_3 treated banana peel	5.8	[44]
Mango peel waste	28.21	[45]
Watermelon peel	20.45	This study

3.9. Comparison with other adsorbents

Table 3 compares the adsorption capabilities (q_{max}) of Zn^{2+} with different adsorbents reported in the literature. While WP used in this work does not undergo any pre-treatment or modification yielded a maximum adsorption capacity of 20.45 mg/g. The value of adsorption capacity in the present work is significantly considerable compared to most other biomasses reported. Thus, the current work revealed that WP is an effective, efficient, economical, renewable, and sustainable adsorbent for removing Zn^{2+} ions from aqueous solutions.

4. Conclusion

We successfully studied the usage of WP as an adsorbent for the removal of Zn^{2+} from an aqueous solution. Langmuir isotherm model could represent the equilibrium data, signifying that the removal of Zn^{2+} follows monolayer and adsorption processes. The maximum monolayer adsorption capacity of WP was 20.45 mg/g. The pseudo-second-order model exhibited that chemical sorption is the rate-limiting step. For the first 10 min, a rapid increase in the adsorption rate of Zn^{2+} onto WP can be observed, accompanied by a less rapid increase and constant plateau after 30 min. The data in the linearized forms of Dubinin–Radushkevich gave satisfactory correlation coefficients for the studied concentrations. Adsorption free energy (E) was estimated at 0.50 kJ/mol, revealing that the physisorption process dominates chemisorption and ion exchange. The results suggest that the WP can be a great candidate as an environmentally friendly and low-cost adsorbent with highly efficient for the adsorption of Zn^{2+}.

Acknowledgement

The authors acknowledge the Faculty of Applied Sciences, Universiti Teknologi (MARA), for providing an Atomic Absorption Spectroscopy, FTIR, and X-ray diffraction (XRD) facility to conduct the analyses.

References

[1] C. Liu, H.H. Ngo, W. Guo, K.-L. Tung, Optimal conditions for preparation of banana peels, sugarcane bagasse and watermelon rind in removing copper from water, Bioresour. Technol., 119 (2012) 349–354.

[2] L.M. Plum, L. Rink, H. Haase, The essential toxin: impact of zinc on human health, Int. J. Environ. Res. Public Health, 7 (2010) 1342–1365.

[3] G. Ringgit, S. Siddiquee, S. Saallah, M.T. Mohamad Lal, A sensitive and rapid determination of zinc ion (Zn^{2+}) using electrochemical sensor based on f-MWCNTs/CS/PB/AuE in drinking water, Sci. Rep., 12 (2022) 18582, doi: 10.1038/s41598-022-21926-6.

[4] H.I. Maarof, W.M.A.W. Daud, M.K. Aroua, Recent trends in removal and recovery of heavy metals from wastewater by electrochemical technologies, Rev. Chem. Eng., 33 (2017) 359–386.

[5] Q. Chen, Y. Yao, X. Li, J. Lu, J. Zhou, Z. Huang, Comparison of heavy metal removals from aqueous solutions by chemical precipitation and characteristics of precipitates, J. Water Process Eng., 26 (2018) 289–300.

[6] J. Cevallos-Mendoza, C.G. Amorim, J.M. Rodríguez-Díaz, M. da Conceição B.S.M. Montenegro, Removal of contaminants from water by membrane filtration: a review, Membranes, 12 (2022) 570, doi: 10.3390/membranes12060570.

[7] R.H. Harharah, G.M.T. Abdalla, A. Elkhaleefa, I. Shigidi, H.N. Harharah, A study of copper(II) ions removal by reverse osmosis under various operating conditions, Separations, 9 (2022) 155, doi: 10.3390/separations9060155.

[8] S. Pan, J. Shen, Z. Deng, X. Zhang, B. Pan, Metastable nano-zirconium phosphate inside gel-type ion exchanger for enhanced removal of heavy metals, J. Hazard. Mater., 423 (2022) 127158, doi: 10.1016/j.jhazmat.2021.127158.

[9] R. Lakshmipathy, N. Sarada, Application of watermelon rind as sorbent for removal of nickel and cobalt from aqueous solution, Int. J. Miner. Process., 122 (2013) 63–65.

[10] S. Meseldzija, J. Petrovic, A. Onjia, T. Volkov-Husovic, A. Nesic, N. Vukelic, Utilization of agro-industrial waste for removal of copper ions from aqueous solutions and mining-wastewater, J. Ind. Eng. Chem., 75 (2019) 246–252.

[11] M. Iqbal, A. Saeed, S.I. Zafar, FTIR spectrophotometry, kinetics and adsorption isotherms modeling, ion exchange, and EDX analysis for understanding the mechanism of Cd^{2+} and Pb^{2+} removal by mango peel waste, J. Hazard. Mater., 164 (2009) 161–171.

[12] N. Islam, A. Habib, A. Islam, A.S. Alam, Removal of copper from aqueous solution using orange peel, sawdust and bagasse, Pak. J. Anal. Environ. Chem., 8 (2007) 6.

[13] M. Hossain, H.H. Ngo, W. Guo, T. Nguyen, Removal of copper from water by adsorption onto banana peel as bioadsorbent, Geomate J., 2 (2012) 227–234.

[14] B.S. Inbaraj, N. Sulochana, Carbonised jackfruit peel as an adsorbent for the removal of Cd(II) from aqueous solution, Bioresour. Technol., 94 (2004) 49–52.

[15] N.S.M. Tahiruddin, R.A. Aziz, R. Ali, N.I. Taib, Potential of using jackfruit peel (*Artocarpus heterophyllus*) as green solution for removal of copper(II) and zinc(II) from aqueous solution: adsorption kinetics, isotherm and thermodynamic studies,

J. Environ. Chem. Eng., 11 (2023) 109953, doi: 10.1016/j.jece.2023.109953.

[16] N.I. Taib, N.A. Rosli, N.I. Saharrudin, N.M. Rozi, N.A.A. Kasdiehram, N.N.T. Abu Nazri, Kinetic, equilibrium, and thermodynamic studies of untreated watermelon peels for removal of copper(II) from aqueous solution, Desal. Water Treat., 227 (2021) 289–299.

[17] Z.M. Shakor, H.H. Mahdi, F. Al-Sheikh, G.M. Alwan, T. Al-Jadir, Ni, Cu, and Zn metal ions removal from synthetic wastewater using a watermelon rind (*Catullus landaus*), Mater. Today Proc., 42 (2021) 2502–2509.

[18] O. Yılmaz, N. Tugrul, Zinc adsorption from aqueous solution using lemon, orange, watermelon, melon, pineapple, and banana rinds, Water Pract. Technol., 17 (2022) 318–328.

[19] D. Castro, N.M. Rosas-Laverde, M.B. Aldás, C.E. Almeida-Naranjo, V.H. Guerrero, A.I. Pruna, Chemical modification of agro-industrial waste-based bioadsorbents for enhanced removal of Zn(II) ions from aqueous solutions, Materials, 14 (2021) 2134, doi: 10.3390/ma14092134.

[20] R. Singh, J.C. Kumar, K.S. Nandpuri, A study on the influence of the structural chemical constituents of the skin of water melon (*Citrullus Lanatus* Sch.) fruit on the incidence of its blossom-end-rot and cracking, Indian J. Hortic., 32 (1975) 98–101.

[21] R. Lakshmipathy, A. Vinod, N. Sarada, Watermelon rind as biosorbent for removal of Cd^{2+} from aqueous solution: FTIR, EDX, and kinetic studies, J. Indian Chem. Soc., 90 (2013) 1147–1154.

[22] A.M. Rimando, P.M. Perkins-Veazie, Determination of citrulline in watermelon rind, J. Chromatogr. A, 1078 (2005) 196–200.

[23] N.A. Reddy, R. Lakshmipathy, N. Sarada, Application of *Citrullus lanatus* rind as biosorbent for removal of trivalent chromium from aqueous solution, Alexandria Eng. J., 53 (2014) 969–975.

[24] A.H. Jawad, Y. Ngoh, K.A. Radzun, Utilization of watermelon (*Citrullus lanatus*) rinds as a natural low-cost biosorbent for adsorption of methylene blue: kinetic, equilibrium and thermodynamic studies, J. Taibah Univ. Sci., 12 (2018) 371–381.

[25] A.H. Jawad, R. Razuan, J.N. Appaturi, L.D. Wilson, Adsorption and mechanism study for methylene blue dye removal with carbonized watermelon (*Citrullus lanatus*) rind prepared via one-step liquid phase H_2SO_4 activation, Surf. Interfaces, 16 (2019) 76–84.

[26] K. Keawkim, A. Khamthip, Removal of Pb^{2+} ion from industrial wastewater by new efficient biosorbents of Oyster plant (*Tradescantia spathacea Steam*) and Negkassar leaf (*Mammea siamensis T. Anderson*), Chiang Mai J. Sci., 45 (2018) 369–379.

[27] T. Phuengprasop, J. Sittiwong, F. Unob, Removal of heavy metal ions by iron oxide coated sewage sludge, J. Hazard. Mater., 186 (2011) 502–507.

[28] N.I. Taib, N. Mohd Aris, Removal of Cd^{2+} from aqueous solution using $MgAlCO_3$-layered double hydroxide, Sci. Res. J., 8 (2011) 13–31.

[29] S. Turkmen Koc, A. Kipcak, E. Moroydor Derun, N. Tugrul, Removal of zinc from wastewater using orange, pineapple and pomegranate peels, Int. J. Environ. Sci. Technol. (Tehran), 18 (2021) 2781–2792.

[30] S. Ben-Ali, I. Jaouali, S. Souissi-Najar, A. Ouederni, Characterization and adsorption capacity of raw pomegranate peel biosorbent for copper removal, J. Cleaner Prod., 142 (2017) 3809–3821.

[31] H. Chen, T. Yan, F. Jiang, Adsorption of Cr(VI) from aqueous solution on mesoporous carbon nitride, J. Taiwan Inst. Chem. Eng., 45 (2014) 1842–1849.

[32] M. Dubinin, The equation of the characteristic curve of activated charcoal, Dokl. Akad. Nauk. SSSR, (1947) 327–329.

[33] D.N. Misra, Adsorption on heterogeneous surfaces: a Dubinin–Radushkevich equation, Surf. Sci., 18 (1969) 367–372.

[34] B.H. Hameed, A.T.M. Din, A.L. Ahmad, Adsorption of methylene blue onto bamboo-based activated carbon: kinetics and equilibrium studies, J. Hazard. Mater., 141 (2007) 819–825.

[35] K. Foo, B. Hameed, Preparation, characterization and evaluation of adsorptive properties of orange peel based activated carbon via microwave induced K_2CO_3 activation, Bioresour. Technol., 104 (2012) 679–686.

[36] B. Hameed, H. Hakimi, Utilization of durian (*Durio zibethinus Murray*) peel as low cost sorbent for the removal of acid dye from aqueous solutions, Biochem. Eng. J., 39 (2008) 338–343.

[37] M.B. Desta, Batch sorption experiments: Langmuir and Freundlich isotherm studies for the adsorption of textile metal ions onto teff straw (*Eragrostis tef*) agricultural waste, J. Thermodyn., 2013 (2013) 375830, doi: 10.1155/2013/375830.

[38] V.J. Inglezakis, A.A. Zorpas, Heat of adsorption, adsorption energy and activation energy in adsorption and ion exchange systems, Desal. Water Treat., 39 (2012) 149–157.

[39] B. Esfandiari, M. Monajjemi, Physical adsorption between mono and diatomic gases inside of carbon nanotube with respect to potential energy, J. Phys. Theor. Chem., 10 (2013) 31–42.

[40] N.I. Taib, N. Kantasamy, S.M. Sumari, N.M. Rafi, Adsorption of Arsenic(V) and Phosphate Onto $MgAlNO_3$-LDHs, 2012 IEEE Symposium on Humanities, Science and Engineering Research, IEEE, Kuala Lumpur, Malaysia, 2012, pp. 333–338.

[41] R.M. Ali, H.A. Hamad, M.M. Hussein, G.F. Malash, Potential of using green adsorbent of heavy metal removal from aqueous solutions: adsorption kinetics, isotherm, thermodynamic, mechanism and economic analysis, Ecol. Eng., 91 (2016) 317–332.

[42] L. Sha, G. Xueyi, F. Ningchuan, T. Qinghua, Adsorption of Cu^{2+} and Cd^{2+} from aqueous solution by mercapto-acetic acid modified orange peel, Colloids Surf., B, 73 (2009) 10–14.

[43] N.-c. Feng, X.-y. Guo, Characterization of adsorptive capacity and mechanisms on adsorption of copper, lead and zinc by modified orange peel, Trans. Nonferrous Met. Soc. China, 22 (2012) 1224–1231.

[44] G. Annadurai, R.-S. Juang, D. Lee, Adsorption of heavy metals from water using banana and orange peels, Water Sci. Technol., 47 (2003) 185–190.

[45] M. Iqbal, A. Saeed, I. Kalim, Characterization of adsorptive capacity and investigation of mechanism of Cu^{2+}, Ni^{2+} and Zn^{2+} adsorption on mango peel waste from constituted metal solution and genuine electroplating effluent, Sep. Sci. Technol., 44 (2009) 3770–3791.